Phase Behavior, Rheology, and Morphology of Binary Blends of Semiflexible Main-Chain Thermotropic Liquid-Crystalline Polymers

Chang Dae Han* and Sukky Chang

Department of Polymer Engineering, The University of Akron, Akron, Ohio 44325

Patrick T. Mather*,†,‡ and Xiaomei Fang†

Polymer Program and Chemical Engineering Department, Institute of Materials Science, University of Connecticut, Storrs, Connecticut 06269

Received November 16, 2000; Revised Manuscript Received June 26, 2001

ABSTRACT: The phase behavior, rheology, and morphology of binary blends of semiflexible main-chain thermotropic liquid-crystalline polymers (TLCPs) were investigated. Specifically, binary blends consisting of poly[(phenylsulfonyl)-*p*-phenylene alkylene-bis(4-oxybenzoate)]s (PSHQ*n*) having five methylene groups (PSHQ5) and 11 methylene groups (PSHQ11) were prepared by solvent casting. It was found from differential scanning calorimetry (DSC) that PSHQ5, PSHQ11, and their blends are glassy thermotropic polymers, exhibiting only glass-to-nematic and nematic-to-isotropic (N−I) transitions. Approximate phase diagrams were constructed for PSHQ5/PSHQ11 blends based on DSC data. Using a cone-and-plate rheometer, transient shear flow experiments were conducted for the PSHQ5/PSHQ11 blends (i) at 160 °C in the biphasic region where PSHQ11 forms an isotropic phase and PSHQ5 forms a nematic phase and (ii) at 130 °C in the nematic region where both PSHQ5 and PSHQ11 formed the nematic phase. It was found for such PSHQ5/PSHQ11 blends that the steady-state shear viscosity at 130 °C (in the nematic region) is lower than that at 160 °C (in the biphasic region). However, the first normal stress difference at 130 °C exhibits a very large overshoot followed by an oscillatory decay until reaching a steady state, while it is virtually zero at 160 °C. The time evolution of morphology for the PSHQ5/PSHQ11 blends, upon shear startup and also upon cessation of shear flow, was investigated using a specially designed optical microrheometer equipped with a polarizing optical microscope. Contrasting observations are reported for the case of nematic PSHQ5 in isotropic PSHQ11 when compared to the nematic PSHQ5/nematic PSHQ11 blend. Shearing of a nematic/nematic blend induces a much larger birefringence change than does shearing a nematic/isotropic blend, and a shear-induced isotropic-to-nematic transition is observed from a mixture of isotropic phases containing two TLCPs.

1. Introduction

A better understanding of the phase behavior and morphology of binary blends of thermotropic liquid-crystalline polymers (TLCPs) can offer an opportunity to obtain new polymeric materials with controlled physical properties. A judicious choice of processing conditions would be extremely important to achieve such a goal. However, like the preparation of any other blends consisting of two homopolymers, miscibility between two TLCPs will be of primary importance when one wishes to prepare binary blends of TLCPs. In the past, some research groups[1−4] investigated miscibility via the exchange reactions (i.e., transesterification) between two TLCPs.

Successful mixing of two chemically dissimilar TLCPs would be challenging, if at all possible. Thus the preparation of binary blends of TLCPs from a homologous TLCP series should yield model compounds. In this regard, a previous study of Watanabe and Krigbaum[1] is worth noting, where a homologous series of semiflexible main-chain TLCPs (PBn) were synthesized with the chemical structure

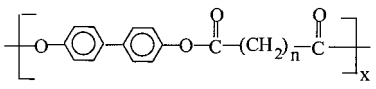

† Polymer Program, University of Connecticut.
‡ Chemical Engineering Department, University of Connecticut.

which is based on 4,4′-dihydroxybiphenyl and various aliphatic diacids. In this study, the chain flexibility was varied through the number of methylene groups (n = 5, 7, 10, and 12) in the flexible spacer, and the phase behavior of binary blends consisting of PB5 and PB7 and consisting of PB10 and PB12 was investigated. Using differential scanning calorimetry (DSC), they found that the PB5/PB7 blends exhibited three transitions during heating, while only two transitions were observed during cooling. Thus, they constructed a phase diagram for the blends from the peak temperatures of exotherms in the DSC cooling curves, revealing a eutectic point at 0.30 mole fraction of PB7 in PB5/PB7 blends and undergoing phase transitions, upon cooling, from the isotropic state to a nematic state and then to a solid state. They noted that each component, PB5 and PB7, crystallized separately during cooling. On the other hand, they obtained a similar phase diagram, whether using the DSC heating curves or the DSC cooling curves, for the PB10/PB12 blends, which underwent, upon cooling, phase transitions from the isotropic state to a smectic state and then to a crystalline solid state.

Previously, Chang and Han[5] synthesized and characterized a homologous series of polyesters, poly[(phenylsulfonyl)-*p*-phenylene alkylene-bis(4-oxybenzoate)s]

10.1021/ma001964d CCC: $20.00
Published on Web 08/21/2001

(PSHQ*n*), with the chemical structure

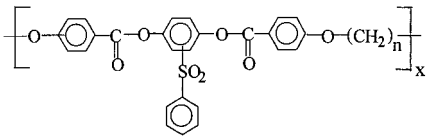

with varying numbers ($n = 3-12$) of methylene groups as flexible spacers. They reported that (i) PSHQ*n* with odd numbers of methylene groups are *glassy* thermotropic polymers, exhibiting only nematic-to-isotropic (N−I) transition, (ii) PSHQ*n* with even numbers of methylene groups are *semicrystalline* thermotropic polymers, exhibiting crystalline-to-nematic and N−I transitions, and (iii) PSHQ3 is an amorphous polyester that exhibits *no* liquid crystallinity. None of the PSHQ*n* polymers was found to exhibit a higher order smectic phase, either on cooling or heating.

In this study, we use PSHQ*n* polymers synthesized previously by Chang and Han[5] to investigate the phase behavior, rheology, and morphology of binary blends consisting of PSHQ5 and PSHQ11. Specifically, (i) the thermal transitions in PSHQ5/PSHQ11 blends were investigated using DSC; (ii) approximate phase diagrams were constructed from the results of DSC and polarizing optical microscopy observations; (iii) the rheological behavior of PSHQ5/PSHQ11 blends in the biphasic and nematic regions was investigated using a cone-and-plate rheometer; and (iv) the time-evolution of morphology for PSHQ5/PSHQ11 blends was investigated using a specially designed optical microrheometer equipped with a polarizing optical microscope, during cooling, upon shear startup, and also upon cessation of shear flow. Because both PSHQ5 and PSHQ11 are *glassy* TLCPs, the PSHQ5/PSHQ11 blends allowed the facile construction of phase diagrams via DSC and investigations, during cooling, of the time evolution of morphology via in situ polarizing optical microscopy without concern for crystallization or cocrystallization. In this paper, we present the highlights of our findings with an emphasis on features unique to blends of two thermotropic polymers.

2. Experimental Section

2.1. Materials and Sample Preparation. In the present study we used PSHQ5 and PSHQ11, which were synthesized previously by Chang and Han,[5] to prepare blends. The rationale behind the choice of the PSHQ5/PSHQ11 blends is that both PSHQ5 and PSHQ11 are glassy thermotropic polymers, exhibiting only N−I transition,[5] greatly simplifying the blend phase behavior. Binary blends of PSHQ5 and PSHQ11 were prepared by dissolving both polymers in dichloromethane and then precipitating rapidly in methanol. For DSC and rheological measurements, specimens with thickness 0.5 mm were prepared by solvent casting in the presence of 0.1 wt % antioxidant (Irganox 1010, Ciba-Geigy Group) and then slowly evaporating the majority of the solvent, first at room temperature in a fume hood for 1 week and then at 80 °C in a vacuum for 3 days to remove any residual solvent.

2.2. Differential Scanning Calorimetry (DSC). Thermal transition temperatures were determined by using a differential scanning calorimeter (Perkin-Elmer, model DSC7) with samples blanketed continuously by a nitrogen atmosphere and employing heating and/or cooling rates of 20 °C/min. The results of the DSC experiments were used to construct phase diagrams.

2.3. Rheological Measurement. An ARES rheometer (Rheometrics Scientific Inc.) with a cone-and-plate fixture (8-mm diameter plate, 0.1 rad cone angle) was used to conduct transient shear flow experiments in which shear stress growth $\sigma^+(t,\dot{\gamma})$ and first normal stress difference growth $N_1^+(t,\dot{\gamma})$ were monitored as functions of time (t) for a fixed shear rate ($\dot{\gamma}$) until reaching a steady state. All experiments were conducted under a nitrogen atmosphere in order to minimize oxidative degradation of the specimen, and the rheometer's temperature control was satisfactory to within ±1 °C. In this study, the rheological behavior of only 20/80 PSHQ5/PSHQ11 and 50/50 PSHQ5/PSHQ11 blends was investigated. As both PSHQ5 and PSHQ11 are glass-forming thermotropic polymers, their blends do not undergo crystallization during cooling from the isotropic state, enabling us to analyze the morphological data of the blends without a complexity that may be caused by the formation of crystals during cooling. Also, the same blends were used to investigate, independently, the time evolution of morphology during cooling from the isotropic state.

2.4. Polarizing Optical Microscopy. Polarizing optical microscopy (POM) observations were conducted in situ during shear using a custom optical rheometer which allows for microscopy observations and/or birefringence measurements during the application of controlled shearing conditions at elevated temperature. The design of this device is described in detail elsewhere.[6,7] Samples with prescribed thickness of 50 ± 2 μm are prepared by first zeroing the gap between the optically flat quartz plates, then separating the plates by 50 μm using the micrometer-based kinematic mount, and finally introducing a thin strand of the cast polymer blend. Annealing under an elevated temperature for up to 30 min was required to achieve the final gap setting, as confirmed by focusing on the top and bottom plates and noting the difference in vertical position. Shearing flow of prescribed shear rate is then applied using a stepper-motor drive to rotate a fine ball screw attached to the upper, translating quartz plate. Static hot-stage POM observations were made using the same equipment, though without shearing. An advantage of this approach over conventional hot-stage POM experiments is a precise knowledge of the sample thickness, enabling fair comparison of textures between samples.

2.5. Spectrographic Birefringence. To quantitatively measure the optical birefringence exhibited by the blends of interest under shear flow conditions, we employ the method of spectrographic birefringence (Δn), developed originally by Hongladoram and co-workers[8] to measure large Δn and subsequently adapted by Mather and co-workers[9] for in situ Δn measurements of thermotropic polymers in flow. In this technique, light from a tungsten halogen lamp is collimated and polarized 45° from the flow axis, passed through the sample (whose plane is perpendicular to the optic axis), and then passed through an analyzer oriented parallel to the polarizer. The light is then collected with a lens and transmitted along a fiber optic cable to a visible-range spectrometer to yield transmission spectra, $T(\lambda)$, related to the sample birefringence through the equation

$$T(\lambda) = A_S \cos^2\left(\pi \frac{\Delta n h}{\lambda}\right) \tag{1}$$

where h is the sample thickness, λ is the optical wavelength, Δn is the birefringence, and A_S is a spectrum envelope amplitude. In our previous paper,[9] we have detailed a discrete Fourier transform method to quickly analyze transmission spectra for the parameters A_S and Δn.

3. Results and Discussion

3.1. Thermal Transition in Binary Blends of PSHQ5 and PSHQ11. Thermal transitions in the PSHQ5/PSHQ11 blend system were investigated using DSC. In running DSC, the following thermal treatments were given to the blend system investigated. PSHQ5/PSHQ11 blends were first heated to 190 °C in the isotropic region and kept there for 3 min, followed by cooling at a rate of 20 °C/min down to 40 °C and then by heating at a rate of 20 °C/min to 190 °C. The

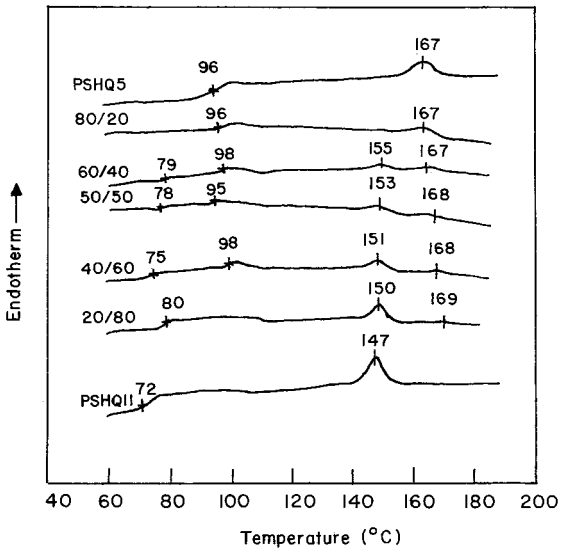

Figure 1. DSC traces during the second heating of PSHQ5/PSHQ11 blends, the compositions of which are given on the DSC traces.

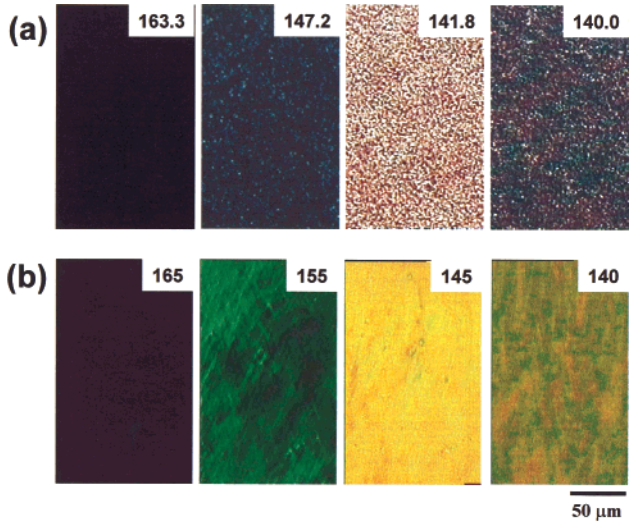

Figure 2. (a) Polarizing optical micrographs observed on cooling a 20/80 PSHQ5/PSH1Q11 blend at a rate of 5 °C/min. (b) Polarizing optical micrographs observed during cooling at 5 °C/min of the 50/50 PSHQ5/PSH1Q11 blend. The temperatures (in celsius) at which each POM image was taken are given on the pictures. Polarizers are crossed with incident polarization oriented along the micrograph horizontal direction. Sample thickness is 50 ± 2 μm.

rationale behind the thermal treatments applied to the each of the blend systems is as follows. First, the initial heating to an isotropic state was necessary to erase previous thermal history associated with the sample preparation. Second, our experimental results, whose details are not presented here, indicated to us that by keeping a binary blend specimen of PSHQ5 and PSHQ11 for only 3 min at a temperature ca. 10−20 °C above the T_{NI} of the constituent components, any discernible transesterification could be avoided. In particular, no alteration in T_{NI} for each component was observed for the thermal history employed.

Figure 1 gives DSC traces for PSHQ5/PSHQ11 blends during the second heating at 20 °C/min. The DSC traces of PSHQ5/PSHQ11 blends appear to be fairly simple, despite the large difference in flexible spacer length, noting that both PSHQ5 and PSHQ11 are glassy TLCPs. Below we will use the peak temperatures of melting endotherms, and midpoints of heat capacity steps, in each DSC curve, given in Figure 1, to determine approximate phase diagrams for the blend system investigated. The results will be discussed below.

Particular attention concerning phase behavior as observed using POM was given to the 20/80 and 50/50 PSHQ5/PSHQ11 blends, as these blends were those selected for both mechanical rheometry and optical rheometry studies. As mentioned above, the PSHQ5/PSHQ11 blends were chosen for the reason that they do not undergo crystallization during cooling, making the analysis of experimental data straightforward. Shown in Figure 2a is a sequence of POM images observed during the cooling of the 20/80 PSHQ5/PSHQ11 blend from 190 to 140 °C at a rate of 5 °C/min. At high temperatures, POM imaging reveals no birefringence, while bright-field microscopy without an analyzer reveals faint inhomogeneity suggesting the presence of two isotropic phases: one that is PSHQ5-rich and the other PSHQ11-rich. On cooling, it is observed that, at $T \sim 153$ °C, the first signs of nematic droplet formation are observed with a droplet size smaller than the isotropic inhomogeneity and a nematic droplet fraction that increases with decreasing temperature. It is noted that T_{NI} for PSHQ5 is near 167 °C, but that significant supercooling of this transition is observed. On continued cooling, a dramatic morphological change is observed near $T = 142$ °C, as the PSHQ11 fraction transforms to a nematic phase so that the entire sample is nematic, although phase-separated into PSHQ5-rich and PSHQ11-rich domains. That two distinct nematic phases coexist is further evidenced by the fact that, on heating, a clear distinction is observed (with POM) between a lower temperature ($T = 147$ °C) and upper temperature ($T = 167$ °C) clearing transition. This is also seen calorimetrically, as reported in Figure 1. On annealing at $T = 140$ °C, where both PSHQ5- and PSHQ11-rich phases are nematic, an optical evolution of *increasing* turbidity is seen until a steady state is quickly reached after about one minute. The increase in turbidity with time—at least temporarily—is opposite the trend observed previously following isotropic−nematic quenching in single component thermotropic polymers[10] and small molecule nematics,[11,12] and its origin is not immediately clear. We speculate that the added interface between coexisting nematic phases may localize regions of enhanced disclination density, thus resulting in increased turbidity as the interface is sharpened with time.

For comparison, we have examined the POM images during similar cooling of the 50/50 PSHQ5/PSHQ11 blend, the results of which are reported in Figure 2b. Again, a relatively slow cooling rate of 5 °C/min was employed to aid in the resolution of morphological transitions. At high temperatures, the absence of transmitted light between crossed polarizers indicates that the blend is optically isotropic. When $T = 155$ °C is reached, a dramatic transition to an optically anisotropic state (nematic) is observed with features distinct from the nematic droplet texture observed in Figure 2a for the 20/80 PSHQ5/PSHQ11 blend. Specifically, a semicontinuous nematic network of PSHQ5-rich phase is detected to appear with a strong tendency toward fibrillar domains, contrasting with the more spherical droplets formed on cooling the 20/80 PSHQ5/PSHQ11 blend to a similar temperature. Moreover, the fibrils appear to have a population of orientations that is

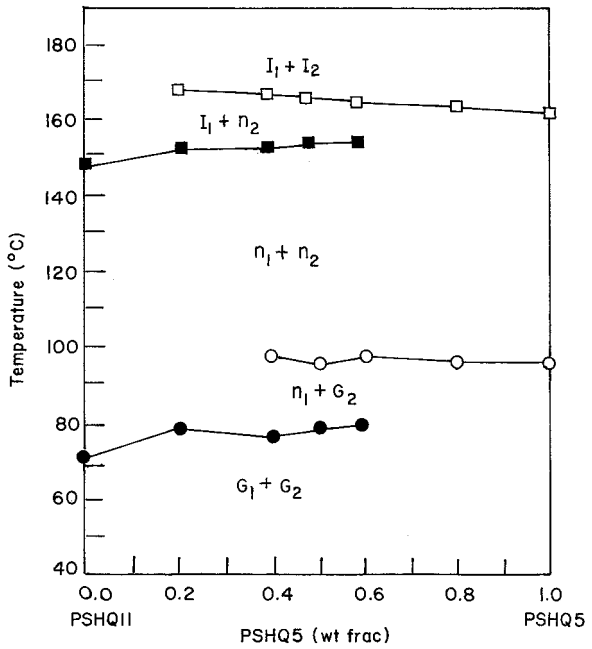

Figure 3. Phase diagrams for PSHQ5/PSHQ11 blends with subscript 1 denoting PSHQ11 and subscript 2 denoting PSHQ5, where I_1 and I_2 denote the isotropic phases of PSHQ11 and PSHQ5, respectively, n_1 and n_2 denote the nematic phases of PSHQ11 and PSHQ5, respectively, and G_1 and G_2 denote the glassy phases of PSHQ11 and PSHQ5, respectively.

biased toward values ±45° relative to the micrograph horizontal. In fact, this apparent morphological bias is an artifact of the optical arrangement chosen for the polarizer (horizontal) and analyzer (vertical) wherein sensitivity to orientations angles $\chi = n\pi/4$ ($n = 1, 3$) with respect to the polarizer are promoted as quantified in the transmission equation for a simple retarder between crossed polarizers

$$I/I_o = \sin^2\left(\pi\frac{\Delta n h}{\lambda}\right)\sin^2(2\chi) \qquad (2)$$

When rotating the crossed polarizers, we observe appearance of fibrils with orientation $\chi = \chi_p + n\pi/4$, where χ_p is the polarizer orientation, with the concomitant fading of fibrils of other orientations.

Continued cooling at 5 °C/min below $T = 155$ °C is observed to lead to increased transmitted intensity, indicating an increase in both the volume fraction of nematic liquid and the local orientation (Δn) within the domains constituting this nematic fraction. Over the range 145 °C > T > 140 °C, a second thermal transition is apparent, as characterized by increased turbidity (decreased transmission) and the appearance of color variations indicative of a spatial modulation in optical retardance. This transition coincides with the second isotropic−nematic transition exotherm detected on cooling in the DSC (not presented here) and is attributed to that of the PSHQ11-rich phase.

3.2. Phase Diagrams for Binary Blends of PSHQ5 andPSHQ11. On the basis of results of thermal transitions described in Figure 1 and POM studies described in reference to Figure 2, an approximate phase diagram was constructed for PSHQ5/PSHQ11 blends, and it is given in Figure 3. In this figure, the phase designations with subscript 1 (e.g., n_1) refers to PSHQ11 and subscript 2 (e.g., n_2) refers to PSHQ5. We wish to point out that the diagrams of Figure 3 should not be regarded as being true equilibrium phase diagrams; in this study, we were not particularly interested in measuring an accurate boundary between different phases. Instead, as will be shown below, our interest in the present study was to investigate the morphology of 20/80 and 50/50 PSHQ5/PSHQ11 blends in the region not very close to the phase boundary. Figure 3 was found to be adequate for this purpose.

Recognizing that PSHQ5 and PSHQ11 are glassy thermotropic polymers,[5] we glean the following information from Figure 3. First, the phase boundary lines are nearly horizontal, showing only slight composition-dependence. As such, we hereafter refer to temperature dependences of the blends as a whole, meaning for all blend compositions. The blends form two isotropic phases, with apparent immiscibility between PSHQ5 and PSHQ11 above the clearing point of each polymer, but each with a detectable concentration of a minor component revealed indirectly with POM. This mixed isotropic state is stable above T_{NI} of PSHQ5 (167 °C). At lower temperatures, the blends form an isotropic/nematic biphase ($I_1 + n_2$), in which an isotropic phase (I_1) of PSHQ11 and a nematic phase (n_2) of PSHQ5 coexist at temperatures 145−150 °C. Still lower in temperature, the blends form an ($n_1 + n_2$) phase, in which the nematic phases of PSHQ11 (n_1) and PSHQ5 (n_2) coexist over the range 95−145 °C. Below the glass transition temperature of PSHQ5 and above that of PSHQ11 (80 °C < T < 100 °C) the blends form nematic/nematic-glass biphase ($n_1 + G_2$), in which a nematic phase (n_1) of PSHQ11 and a glassy phase (G_2) of PSHQ5 coexist, although the glass transition event for PSHQ5 is difficult to detect for low weight fractions of PSHQ5. Finally, the blends form a nematic-glass/nematic-glass biphase ($G_1 + G_2$), in which a glassy phase of PSHQ11 (G_1) and a glassy phase of PSHQ5 (G_2) coexist at temperatures below 77 °C (the T_g of PSHQ11). The phase diagram of PSHQ5/PSHQ11 blends looks relatively simple in that there is no crystalline phase in the blends, owing to the nematic vitrification of the component polymers. We only speculate that the difference in flexible spacer length between the component polymers in the PSHQ5/PSHQ11 blends is sufficiently large, giving rise to the difference in T_{NI} between the component polymers as much as to 21 °C, and consequently the PSHQ5/PSHQ11 blends are not miscible in the nematic state.

It is appropriate at this juncture to compare the phase diagrams presented in Figure 3 with the phase diagrams reported earlier by Watanabe and Krigbaum,[1] who employed binary blends of PB5 and PB7, and binary blends of PB10 and PB12 (the chemical structures of PB*n* appear in the Introduction Section of this paper). The phase diagrams for the PB5/PB7 blends reported by Watanabe and Krigbaum represent blend behavior far more complicated than that of the PSHQ5 PSHQ11 blends presented in Figure 3 above. Interestingly, Watanabe and Krigbaum found that the PB10/PB12 blends underwent smectic-to-isotropic (S−I) transition.

The fact that the PB*n* moieties investigated by Watanabe and Krigbaum[1] exhibit an S−I transition indicates that they have more ordered molecular packing compared to the PSHQ*n* moieties exhibiting only N−I transition. In a previous paper, Chang and Han[13] reported that poly[*p*-phenylene alkylene bis(4-oxybenzoate)] (PHQ*n*)

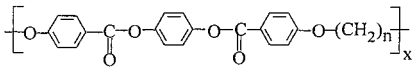

with $n = 10$ exhibited both smectic-to-nematic (S−N) and N−I transitions, a complication avoided in the present blend studies through the use of phenylsulfonyl substitution.

3.3. Rheological Behavior of Binary Blends of PSHQ5 and PSHQ11. Transient and steady-state shear flow behavior of 20/80 and 50/50 PSHQ5/PSHQ11 blends were investigated. The primary reason for the choice of the particular blends for our rheology study was based on our interesting hot-stage morphology observations made using the same binary blends of PSHQ*n* during cooling from the isotropic state and described in Section 3.1, above. Later in this paper, we will present in situ polarizing optical micrographs for PSHQ5/PSHQ11 blends, which were taken during flow inception at various temperatures.

As pointed out previously by Han and co-workers,[14−18] the reproducibility of rheological measurements for TLCPs is nontrivial, yet very essential, and they established procedures whereby reproducible rheological data can be obtained for TLCPs. Following such procedures, in this study we have taken the following steps for rheology measurements for 20/80 and 50/50 PSHQ5/PSHQ11 blends. A specimen was inserted into the cone-and-plate fixture of an ARES rheometer, which had been heated to 200 °C in the isotropic region, allowing expedited relaxation of sample loading stresses, and then sheared there at a shear rate ($\dot{\gamma}$) of 0.5 s^{-1} for 2 min (60 strain units). The specimen was then cooled slowly down to 160 or 130 °C, where 1 h was allowed for thermal equilibration, after which a sudden shear flow was applied to the specimen at $\dot{\gamma} = 0.5$ s^{-1} for 1 h (1800 strain units). During the entire 1-h period, growths in shear stress $\sigma^+(t,\dot{\gamma})$ and first normal stress difference $N_1^+(t,\dot{\gamma})$ were recorded.

Shear start-up behavior of 20/80 and 50/50 PSHQ5/PSHQ11 blends reveals interesting temperature and composition dependences. Figure 4 gives plots of $\sigma^+(t,\dot{\gamma})$ vs shear strain ($\dot{\gamma}t$), upon shear startup followed by a steady state, at 160 and at 130 °C for (a) 20/80 PSHQ5/PSHQ11 blend and (b) 50/50 PSHQ5/PSHQ11 blends. According to Figure 3, at 160 °C both blends are in the $(I_1 + n_2)$ biphasic region, and at 130 °C both blends are in the $(n_1 + n_2)$ nematic region. The following observations are worth noting in Figure 4. At 160 °C the shear stress of both blends exhibits a very mild overshoot and then reaches a steady state rather quickly. However, at 130 °C the shear stress of both blends exhibits a very large overshoot followed by a rapid decay initially with some oscillations, and a very slow subsequent decay. It is interesting to observe in Figure 4 that at 130 °C both blends hardly attain a steady state even at $\dot{\gamma}t = 1800$ (i.e., after 1 h upon shear startup). Previously, Chang and Han[18] reported that upon shear startup at $\dot{\gamma} = 0.5$ s^{-1}, the shear stress of PSHQ5 at 150 °C attained a steady state at $\dot{\gamma}t \approx 100$. Such a large difference in strain required to attain a steady-state shear stress between 20/80 PSHQ5/PSHQ11 blend or 50/50 PSHQ5/PSHQ11 blend and neat PSHQ5 can be attributed to the existence of two nematic mesophases, one from PSHQ5 and the other from PSHQ11. At this juncture we only speculate that a blend of the two nematic mesophases might require significant shearing to yield a steady morphology, deferring detailed discussion to our in situ morphology study discussed in Section 3.4, below.

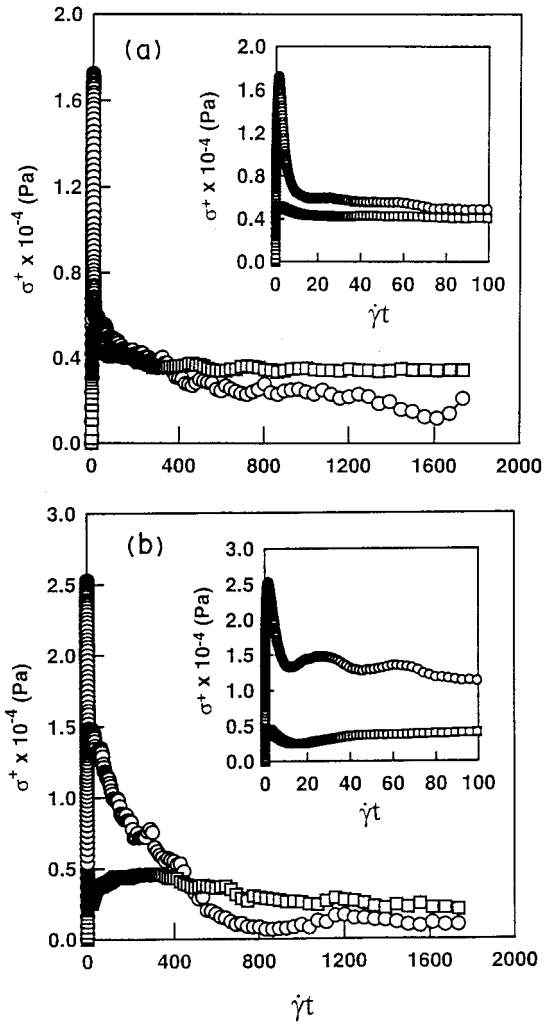

Figure 4. (a) Variations of $\sigma^+(t,\dot{\gamma})$ with $\dot{\gamma}t$ during startup shear flow at $\dot{\gamma} = 0.5$ s^{-1} for the 20/80 PSHQ5/PSH1Q11 blend at 160 °C in the $(I_1 + n_2)$ region (□) and at 130 °C in the $(n_1 + n_2)$ region (○). (b) Variations of $\sigma^+(t,\dot{\gamma})$ with $\dot{\gamma}t$ during startup shear flow at $\dot{\gamma} = 0.5$ s^{-1} for the 50/50 PSHQ5/PSH1Q11 blend at 160 °C in the $(I_1 + n_2)$ region (□) and at 130 °C in the $(n_1 + n_2)$ region (○). Refer to Figure 3 for the phase diagram of the PSHQ5/PSHQ11 blends.

Notice further in Figure 4 that the shear stresses at 160 and 130 °C cross each other at $\dot{\gamma}t \approx 400$, indicating that the viscosity of the 20/80 and 50/50 PSHQ5/PSHQ11 blends at 130 °C in the $(n_1 + n_2)$ nematic region is lower than that at 160 °C in the $(I_1 + n_2)$ biphasic region. This is not surprising in that previously Kim and Han[19] showed that the shear viscosities of PSHQ10 were lower in the nematic region than in the biphasic region. They attributed the experimental observation to substantial orientation, under shear flow, of the anisotropically arranged macromolecules in the nematic phase, which gives rise to a lower resistance to flow compared to the randomly distributed chain conformation of the isotropic phase. What is most interesting in Figure 4 is the long time behavior: an erroneous conclusion that the viscosities of the 20/80 and 50/50 PSHQ5/PSHQ11 blends were lower at 160 °C than at 130 °C would have been reached *if* we had not run the experiment for a sufficiently long time (i.e., $\dot{\gamma}t > 400$).

Figure 5 gives plots of $N_1^+(t,\dot{\gamma})$ vs $\dot{\gamma}t$, upon shear startup followed by a steady state, at 160 °C in the $(I_1$

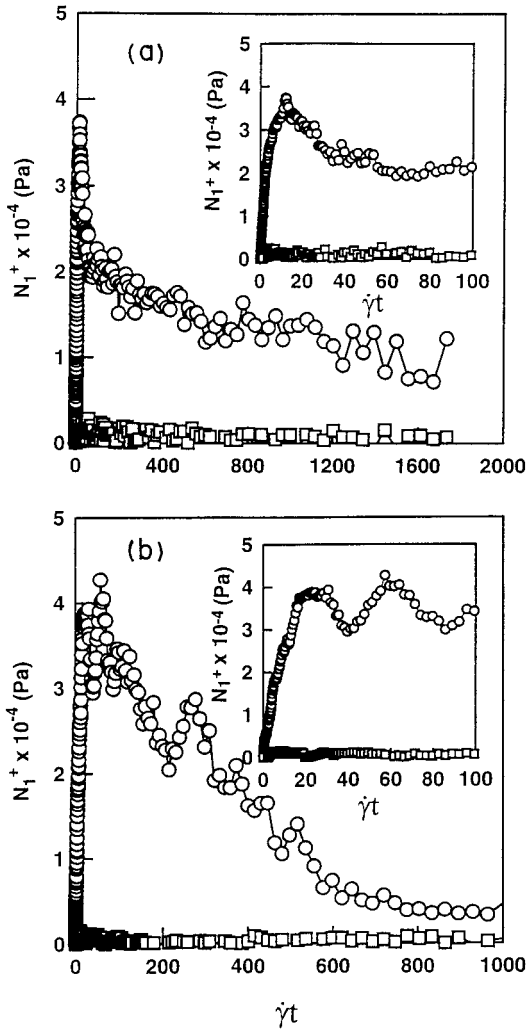

Figure 5. (a)Variations of $N_1^+(t,\dot{\gamma})$ with $\dot{\gamma}t$ during startup shear flow at $\dot{\gamma} = 0.5$ s^{-1} for the 20/80 PSHQ5/PSHQ11 blend at 160 °C in the ($I_1 + n_2$) region (□) and at 130 °C in the ($n_1 + n_2$) region (○). (b) Variations of $N_1^+(t,\dot{\gamma})$ with $\dot{\gamma}t$ during startup shear flow at $\dot{\gamma} = 0.5$ s^{-1} for the 50/50 PSHQ5/PSH1Q11 blend at 160 °C in the ($I_1 + n_2$) region (□) and at 130 °C in the ($n_1 + n_2$) region (○). Refer to Figure 3 for the phase diagram of the PSHQ5/PSHQ11 blends.

+ n_2) biphasic region, and at 130 °C in the ($n_1 + n_2$) nematic region for (a) 20/80 PSHQ5/PSHQ11 blend and (b) 50/50 PSHQ5/PSHQ11 blend. The following observations are worth noting in Figure 5. Values of $N_1^+(t,\dot{\gamma})$ at 160 °C are virtually zero for both blends. This is interpreted as being the situation where at 160 °C both blends form an emulsion, in which the nematic phase of PSHQ5 is suspended in the Newtonian fluid of PSHQ11. At 130 °C both blends exhibit a very large overshoot followed by a rapid decrease with oscillations. Earlier, Han and co-workers,[14−17] who investigated transient shear flow of PSHQ10 in the nematic state, reported similar observations. It is interesting to observe in Figure 5b that the $N_1^+(t,\dot{\gamma})$ for the 50/50 PSHQ5/PSHQ11 blend exhibits a second overshoot, the size of which is even greater than the size of the first overshoot. Such an observation was not made for *neat* PSHQ*n* in the previous studies of Han and co-workers.[14−18] On the other hand, in Figure 5a, we observe a single, very large overshoot in $N_1^+(t,\dot{\gamma})$ for the 20/80 PSHQ5/PSHQ11 blend, similar to those reported for neat PSHQ*n*.[14−18] In other words, the transient shear flow behavior of the 50/50 PSHQ5/PSHQ11 blend is quite different from that

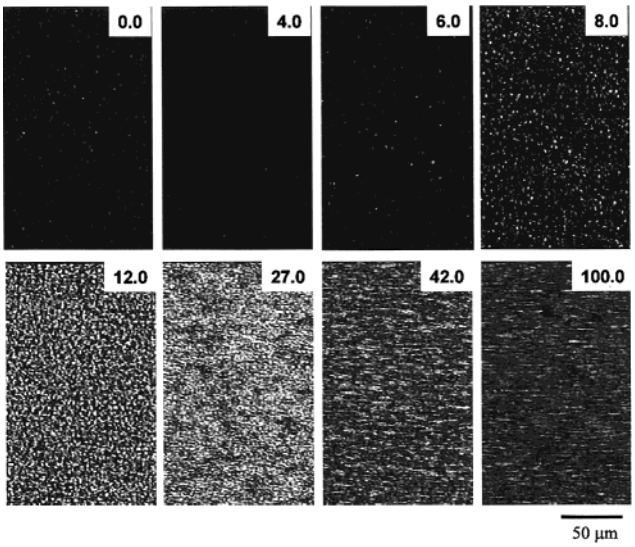

Figure 6. Sequence of polarizing optical micrographs during the shear flow of a 20/80 PSHQ5 PSHQ11 blend at a shear rate of 0.5 s^{-1} and a temperature of 160 °C. The times for each image, in seconds following the onset of shearing, are indicated in the upper right-hand of each image. The polarizers are crossed and oriented with the polarizer at an angle of 45° with respect to the flow axis and the flow is from right to left.

of the 20/80 PSHQ5/PSHQ11 blend. The origin of such a difference is presently not clear, but requires further investigation in the future. However, when presenting below the results of our investigation on the time evolution of morphology of PSHQ5/PSHQ11 blends, we will shed some light on this subject.

3.4. Time Evolution of the Morphology of PSHQ5/PSHQ11 Blends under Shear. To complement the rich mechanical rheometry results reported in Figures 4 and 5 for blends of PSHQ5 and PSHQ11, we have employed novel methods of optical microrheometry in which thin films are sheared between heated quartz disks and observations made using POM and quantitative birefringence. For direct comparisons, the thermal and flow protocol (except for total strain units applied) employed for Figures 4 and 5 above were reproduced. In all cases, unless otherwise specified, the sample thickness is 50 ± 2 μm and the crossed polarizers are rotated at an angle $\pi/4$ with respect to the (horizontal) flow axis.

Shown in Figure 6 is a time sequence of POM micrographs for the 20/80 PSHQ5/PSHQ11 blend sheared at $T = 160$ °C and at a shear rate, $\dot{\gamma} = 0.5$ s^{-1}. Time, in seconds, is indicated in each micrograph. As was the case for Figure 4 (open squares), this temperature corresponds to that for a nematic PSHQ5-rich phase dispersed in a matrix of an isotropic PSHQ11-rich phase. At $t = 0$, it is seen that the morphology consists primarily of nematic (birefringent) droplets in an isotropic matrix. We note that no preferential bias of the nematic orientation within these PSHQ5 domains is anticipated, thus the population of droplets whose internal director orientations are along the microscope's optic axis (velocity gradient direction of the flow cell) or oriented parallel to either the polarizer or analyzer (see eq 1) are not visible due to polarization extinction by the analyzer. Immediately following application of flow ($\dot{\gamma}t \sim 2$ strain units), we consistently observe a *darkening* of the nematic domains, but this transient morphology is quickly supplanted ($\dot{\gamma}t \sim 3$ strain units) by one similar to the quiescent structure, though with

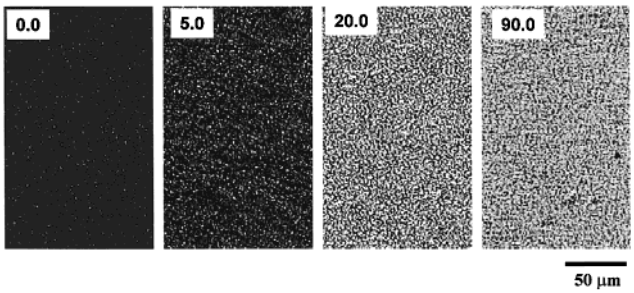

Figure 7. Sequence of polarizing optical micrographs during the shear flow of a 20/80 PSHQ5/PSHQ11 blend at a shear rate of 0.5 s^{-1} and a temperature of 140 °C. The times in seconds following flow inception are indicated for each image. The polarizers are crossed and oriented with the polarizer at an angle of 45° with respect to the flow axis, and the flow is from left to right.

enhanced contrast between the nematic domains—now with higher orientation—and the isotropic background. Continuing the steady shearing at $\dot{\gamma} = 0.5\ s^{-1}$ leads to an apparent *phase inversion* from a continuous isotropic phase at 3 strain units to a continuous nematic phase, the transition occurring over the range of accumulated strains, $4 < \dot{\gamma}t < 6$ strain units. At this stage, ($\dot{\gamma}t > 6$ strain units), it becomes impossible to distinguish the existence (or not) of any isotropic phase, as the shear-induced phase inversion leads to a nematic "masking" of any still-existing isotropic regions. Nonetheless, rheological data ($N_1^+(t,\dot{\gamma})$, Figure 5) suggest the continued predominance of isotropic material. Finally, continued steady shearing of this blend for $12 < \dot{\gamma}t < 50$ strain units results in domain size coarsening with a gradual transformation from a pale white texture, indicating small domains sampling a large number of director orientations (colors), to a uniform aqua color superposed with white patches (of continually decreasing area fraction) indicating a trend toward locally uniform, near-monodomain, director alignment.

Although the experiment just described was halted at this stage due to experimental limitations, it is clear in observing the trend in sample morphology with increasing strain that the morphological transformations are continuing to occur at an accumulated strain of 50 strain units. By extrapolation of the image sequence in Figure 6, we might expect or predict that the final steady state texture (achieved only near $\dot{\gamma}t \sim$ 400 strain units per Figure 4) would be a homogeneous aqua color suggesting uniform birefringence. That the trend is toward a homogeneous morphological state implicates a flow-induced *mixing* that may begin to occur for $\dot{\gamma}t > 12$ strain units. As this phase is apparently birefringent, is it possible that the PSHQ11-rich phase is induced into a nematic phase; i.e., a flow-induced isotropic−nematic transition? Recalling that the quiescent $T_{NI} = 147$ °C, $\Delta T = T_{NI} - T = 13$ °C, which according to previous results[7] on PSHQ10 of comparable molecular weight (and viscosity) a critical shear rate, $1 < \dot{\gamma}_{cr} < 2\ s^{-1}$, is required to induce the nematic phase. Thus, this explanation seems plausible, although direct proof of this possibility is beyond the scope of the present investigation.

We have examined, also, the contrasting morphological evolution of the 20/80 PSHQ5/PSHQ11 blend at a lower temperature, $T = 140$ °C, where both phases are completely nematic. A representative POM sequence for these experimental conditions is shown in Figure 7 for the strain range $0 < \dot{\gamma}t < 50$ and had the same optical arrangement that was used for Figure 6. To aid in distinguishing the two phases, we exploit the finding that the second material to undergo the isotropic−nematic transition on cooling (PSHQ11) is significantly more turbid than the first (PSHQ5), a fact likely due to the higher disclination density associated with a shorter coarsening time. Thus, the first micrograph in Figure 7 features a morphology with a dark background and a bright dispersed phase, the former determined to be PSHQ11-rich by imaging over a range of incident intensities while cooling. On inception of steady shearing flow, a slight brightening and stretching of the dispersed (PSHQ5-rich) phase is observed, accompanied by no substantial changes to the matrix fluid. Further shearing, however, leads to dramatic morphological changes in which the overall brightness and retardance homogeneity increase substantially. This transition indicates orientation and coarsening of both phases—especially the PSHQ11-rich matrix that was initially quite turbid—and occurs over the strain range $5 < \dot{\gamma}t < 10$. Beyond 18 strain units, the morphology achieves an apparent steady state, although the experiment was terminated after the accumulation of 50 strain units. We find that the transformation of the turbid PSHQ11-rich matrix to an oriented, clear, fluid is long-lived, even following the removal of flow.

In comparison with the mechanical rheometry data of Figures 4 ($\sigma^+(t)$) and 5 ($N_1^+(t,\dot{\gamma})$), the morphological transformation observed in Figure 7 appears to be most correlated with the strong $N_1^+(t,\dot{\gamma})$ overshoot for the same conditions as shown most clearly in the inset of Figure 5. This sensitivity of normal stress data to morphological changes in sheared LCPs has been reported previously by Mather et al.[9] and Kim et al.[20] on similar polymers and by other researchers working on flow inception of immiscible polymer blends.[21,22] Presumably, the continued gradual decay in $N_1^+(t,\dot{\gamma})$ shown in Figure 5 would be accompanied by continued coarsening of the morphologies shown in Figure 7, were these large strain rheo-optical observations possible.

The evolution of blend microstructure was also examined for the 50/50 PSHQ5/PSHQ11 blend, revealing unique features deserving description. Referring to Figure 2b, it was observed for this blend that, when cooling at 5 °C/min, no evidence of a nematic PSHQ5-rich phase was evident until $T \sim 155$ °C. However, annealing at $T = 160$ °C for more than several minutes, a temperature below the equilibrium clearing transition of $T = 168$ °C, a diffuse nematic morphology shown as the first micrograph in Figure 8 emerges. Rotation of the crossed polarizers from the 45°/135° orientation employed in Figure 8 reveals that the dark regions are indeed birefringent (nematic), not isotropic. Thus, the nematic + isotropic morphology of the 50/50 PSHQ5/PSHQ11 blend is strikingly similar to the nematic texture observed for such lyotropic LCPs as poly(benzyl glutamate)[23,24] and poly(*n*-hexyl isocyanate).

On applying steady shear flow, Figure 8 reveals a significant brightening with increasing accumulated strain, yet with the maintenance of a diffuse, lyotropic-like microstructure characterized by a large characteristic correlation length, $a \approx 30-40\ \mu$m. We note that some transient band formation is observed over the strain range $7.5 < \dot{\gamma}t < 10$ but that from experiment to experiment the details of their emergence and structure varies significantly with apparent sensitivity to the local orientation state and its history.

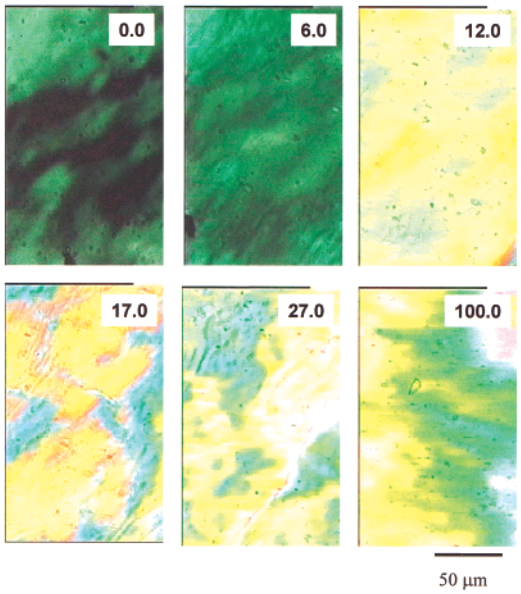

Figure 8. Sequence of polarizing optical micrographs during the shear flow of a 50/50 PSHQ5/PSHQ11 blend at a shear rate of 0.5 s^{-1} and a temperature of 160 °C. The polarizers are crossed and oriented with the polarizer at an angle of 45° with respect to the flow axis, and the flow is from left to right. The times in seconds following flow inception are indicated for each image.

That the morphologies of Figure 8 so closely resemble those of commonly studied lyotropic LCPs suggests the possibility of a submicrometer microstructure that we now describe. For length scales smaller than our optical resolution, the nematic PSHQ5 exists in the forms of *anisotropic domains* containing one or more molecules—likely the latter—that, themselves, align as a lyotropic nematic phase in the PSHQ11 "solvent". We believe that the domains are finite in size, containing a large number of PSHQ5 chains, based on the DSC and hot-stage POM observations that the clearing transition of this "homogeneous" nematic phase is close to that of neat PSHQ5. Also, the existence of such small domains may be energetically allowed only for diminishingly small interfacial tension between PSHQ5 and PSHQ11, which is not unreasonable for such chemically similar species. It is noted that previous evidence for the formation of a lyotropic mesophase by an aromatic polyester in an isotropic polymeric "solvent" was reported by Kricheldorf and co-workers,[25] where up to 8 wt % of an all-aromatic rodlike polyester was codissolved with poly(ϵ-caprolactone) (PCL) in a solvent and coprecipitated in a nonsolvent. Such materials yielded a birefringent mobile phase (i.e., liquid crystalline phase) like that observed by us in Figure 8 for temperatures between the melting point of PCL and the much higher melting point of the rigid-rod polyester. The authors infer that the liquid crystallinity results from alignment of highly anisotropic *solid* domains of the rigid rod polyester in PCL, a mechanism distinct from ours in which the nematogen (PSHQ5) is itself nematic, not crystalline. We seek in the future to test this dimension hypothesized morphology using small-angle X-ray scattering to look for aligned objects of dimension 10−100 nm.

Following cessation of shear at T = 160 °C, the oriented morphology of the 50/50 PSHQ5/PSHQ11 blend relaxes quite rapidly, as shown in Figure 9. In particular, the trend with time is toward lower retardances (considering the inverse progression along Newton's color sequence) with increasing heterogeneity of the

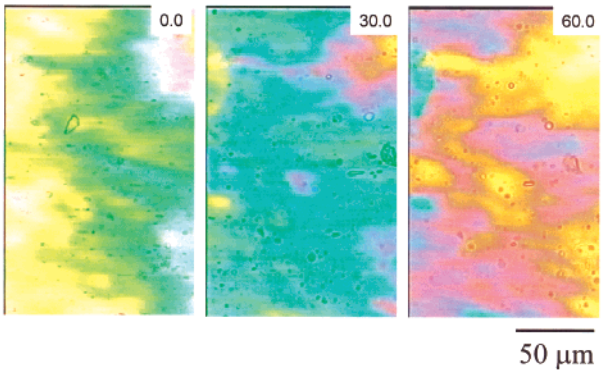

Figure 9. Sequence of polarizing optical micrographs taken following cessation of steady shearing of a 50/50 PSHQ5/PSHQ11 blend at a shear rate of 0.5 s^{-1} and a temperature of 160 °C for observation times of 0, 30, and 60 s following the cessation of flow.

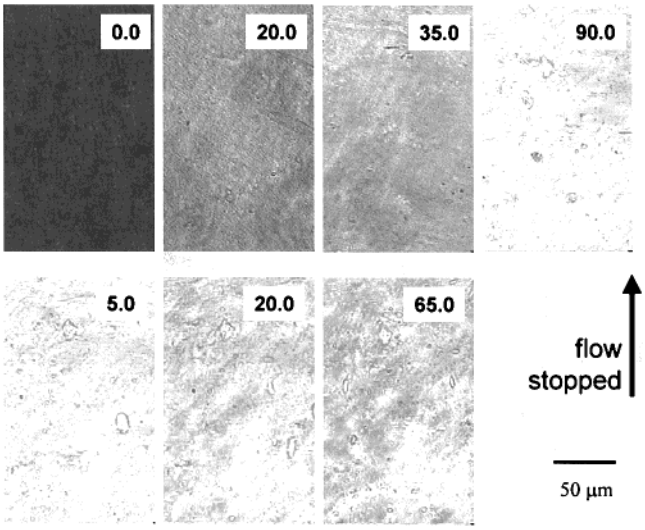

Figure 10. Sequence of polarizing optical micrographs during the shear flow, and following flow cessation after 50 strain units, of a 50/50 PSHQ5/PSHQ11 blend at a shear rate of 0.5 s^{-1} and a temperature of 140 °C. The times during shear and annealing time in seconds following shear are indicated in the upper right-hand of each image. The polarizers are crossed and oriented with the polarizer at an angle of 45° with respect to the flow axis and the flow is from left to right.

sample orientation. After 1 min of annealing, for example, the POM image reveals a wide range of retardance colors separated over the range 10−20 μm. More quantitative birefringent mapping is presently not possible, but we are developing methods to achieve this needed mapping.

At a lower temperature, T = 140 °C, both the PSHQ5- and PSHQ11-rich phases are completely nematic and the 50/50 PSHQ5/PSHQ11 blend exists as a very fine ($a \sim 1$ μm), turbid microdomain texture as shown in Figure 10 for t = 0. Application of steady shearing with $\dot{\gamma}$ = 0.5 s^{-1} leads to a monotonic decrease in sample turbidity and an increase in apparent domain size until t = 50−60 s ($25 < \dot{\gamma}t < 30$). At that stage, a uniformly bright and coarse nematic texture is observed. We do note that, at early stages, ($\dot{\gamma}t < 5$) some collective domain orientation appears to be biased along the vorticity axis—akin to transient banding—only to give way to a more uniform texture at higher strains. In contrast to the lack of orientational stability following flow of the same blend at T = 160 °C, Figure 10 reveals only small changes to the orientation state of the blend

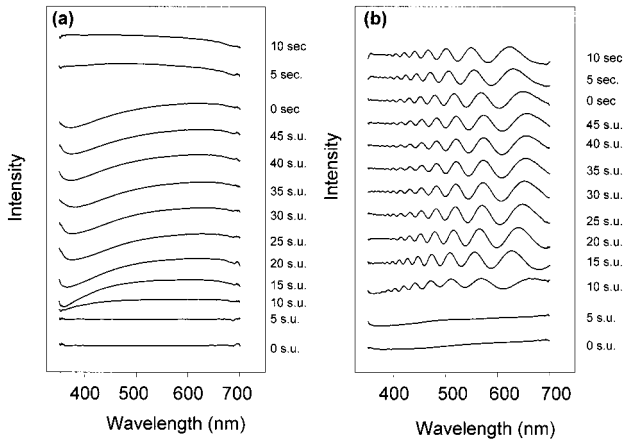

Figure 11. Parallel polarizer transmission spectra for a 50/50 PSHQ5/PSHQ11 blend at a shear rate of 0.5 s^{-1} and a temperature of (a) 140 °C compared to (b) 160 °C. Parallel polarizers were oriented 45° from the flow axis. A sample thickness of 50 ± 2 μm was used.

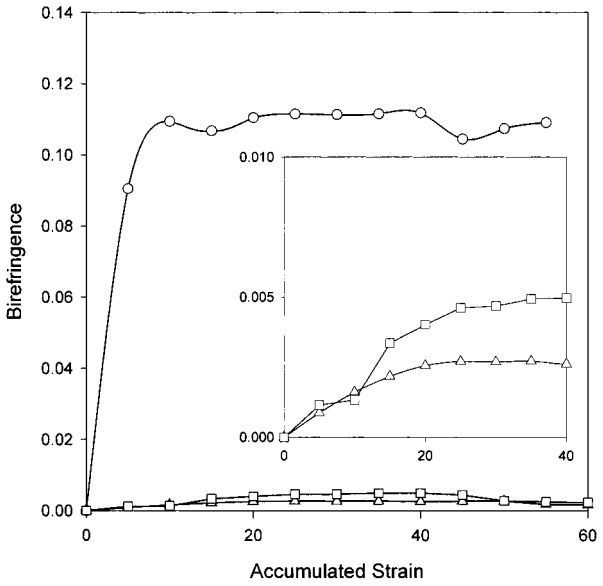

Figure 12. Spectrographic birefringence computed from the transmission spectra of Figure 11 for the 50/50 PSHQ5/PSHQ11 blend sheared for 50 strain units at 0.5 s^{-1} at 140 °C (○) and at 160 °C (△) and for a shear rate of 2.5 s^{-1} at T = 160 °C (□).

for the first minute following flow cessation. Further annealing leads to only minor refinement of the texture shown for t = 65 s in Figure 10. Comparing the morphology evolution prior to flow cessation with the normal stress growth data in Figure 5 indicates that no obvious morphological origin exists for the observed double $N_1^+(t, \dot{\gamma})$oscillation unique to this blend. Thus, these peaks may arise from dynamics of structures smaller in length scale than those probed with POM; i.e., $a < 1$ μm, including the dynamics of individual molecules.

We can now compare the steady-state POM morphologies of Figures 8 and 10 for the 50/50 PSHQ5/PSHQ11 blend at T = 160 and 140 °C, respectively. At first glance, the steady-state morphologies observed for this blend appear to be similar, with some increased orientation and orientation stability after flow observed for the case T = 140 °C, where both PSHQ5 and PSHQ11 are nematic. To quantify our comparison of these apparently similar flow orientations, we have employed in situ spectrographic birefringence measurements. The results are shown in Figure 11 for (a) T = 160 °C and (b) T = 140 °C, to be compared with the POM sequences of Figures 8 and 10, respectively. In these figures, the spectra have been vertically displaced for clarity with all data being plotted over the same scale, $0 < T(\lambda) < 100\%$. The transmission spectra quickly reveal a disparity in orientation states that is more dramatic than we initially inferred from POM micrographs. In particular, we observe that, at T = 160 °C, only a single depression in $T(\lambda)$ are observed, which, according to eq 1, indicates a steady retardance, $\Delta nh \leq 600$ nm. On the other hand, Figure 11b reveals that shearing the nematic/nematic blend at the same shear rate leads to multiple oscillation in the transmission spectrum indicating substantially larger retardances at steady state, $\Delta nh \geq 600$ nm. In both cases, an apparent steady state for birefringence (and thus retardance) growth is reached quite quickly—within 25 strain units—while the nematic/isotropic blend shows rapid relaxation to an unoriented state in contrast with the nematic/nematic blend revealing only subtle orientational relaxation. These spectra are thus in agreement with the qualitative POM observations made under the same conditions. Analyzing the spectra of Figure 11 allows the extraction of $\Delta n^+(t,\dot{\gamma})$ data, reported in Figure 12, revealing quantitatively the large difference in steady-state orientations under the two conditions, along with a higher shear rate for T = 160 °C. For T = 140 °C and $\dot{\gamma} = 0.5$ s^{-1}, we observe a rapid increase in birefringence from zero to $\Delta n = 0.112$ after a strain of 25 strain units has accumulated, while at T = 160 °C, a steady-state birefringence nearly 2 orders of magnitude smaller is observed, $\Delta n = 0.0027$. At a higher shear rate of $\dot{\gamma}$ = 2.5 s^{-1}, the steady-state birefringence is about doubled, as can be clearly seen in the expanded inset figure, achieving a level of $\Delta n \sim 0.005$. Thus, despite our assessment of comparable steady-state orientation states gleaned from Figures 8 and 10, quantitative analysis has revealed a dramatic—40-fold—difference in birefringence for the nematic/nematic blend when compared to the more weakly oriented nematic/isotropic blend at the same shear rate.

This difference parallels favorably the contrast in observed normal stress data of Figure 5b where the nematic/nematic 50/50 PSHQ5/PSHQ11 blend, for low strains, is observed to feature large positive normal stresses, indicative of fluid elasticity, while the nematic/isotropic blend showed no evidence for normal stress development at the same shear rate. We conclude, therefore, that the elasticity observed for the 50/50 PSHQ5/PSHQ11 blend at T = 160 °C is strongly related to the existence of substantial orientational ordering as manifested in optical birefringence data.

Finally, we have examined the possibility of inducing a flow-induced isotropic−nematic transition for a temperature, T = 180 °C, for the 20/80 PSHQ5/PSHQ11 blend where both components are isotropic, but not intimately mixed. Our interest in this possibility stems from our previous observations[7] on a flow-induced isotropic−nematic transition for isotropic PSHQ10 exposed to shearing flow of sufficient strength. Unique to the present investigation is the added complication of two components, existing as separate isotropic phases, where only one component—PSHQ5—has a propensity toward nematic phase formation due to the proximity of the test temperature (180 °C) to the quiescent isotropic−nematic transition temperature (168 °C). We have found that, indeed, direct POM observations reveal the existence of a critical shear rate, above which

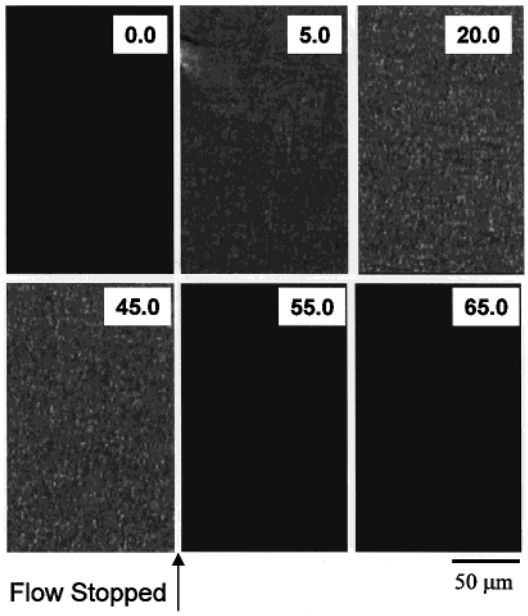

Figure 13. Sequence of polarizing optical micrographs during the shear flow of a 20/80 PSHQ5/PSHQ11 blend at a shear rate of 0.5 s^{-1} and a temperature of 180 °C, where each material is isotropic at rest. The times for each image, in seconds following the onset of shearing, are indicated in the upper right-hand of each image. The polarizers are crossed and oriented with the polarizer at an angle of 45° with respect to the flow axis, and the flow is from left to right.

nematic droplets form within and otherwise isotropic matrix and below which only slight flow birefringence is observed. Figure 13 shows a sequence of POM images for the case where the critical shear rate is exceeded and nematic droplets are formed, namely $\dot{\gamma} = 1.0\ s^{-1}$. In this figure, the times following flow inception are shown in seconds and the total strain prior to cessation was 50 strain units. Here, we see that after the accumulation of 20 strain units, a fully developed microstructure appears in which small birefringent droplets of size 5−20 μm, roughly spherical in shape, are suspended in a dark, isotropic matrix. Within five seconds following the cessation of flow, the nematic PHSQ5 droplets completely "melt" to the isotropic phase, leaving a dark and homogeneous POM micrograph as shown in Figure 13. Although we have not yet studied the concomitant rehomogenization of such a PSHQ5 and PSHQ11 into a single phase, presumably using small angle light scattering (SALS), such a study would be quite revealing concerning the degree of compatibility and diffusion rate. At lower shear rates, $\dot{\gamma} < 1.0\ s^{-1}$, no clear formation of nematic droplets is evidenced; instead, only a homogeneous and weak brightening is observed following the stress-optical relation common to all isotropic molten polymers.

4. Concluding Remarks

In the present study, we have used DSC analyses to construct approximate phase diagrams for blends of semiflexible main-chain TLCPs as model polymers having different flexible spacer lengths. The phase diagrams enabled us to determine the blend compositions at which further investigations of the rheological behavior and phase morphology might be warranted.

The rheological behavior of a blend consisting of two TLCPs can be very complicated depending upon the morphology of such blends. In this paper, we have demonstrated that a good understanding of the phase behavior of binary blends of TLCPs is essential for a meaningful investigation of the rheological behavior of such blends. In other words, rheology−morphology relationships must be established in order to correctly interpret rheological measurements. For this reason, in the present study, we also conducted an independent investigation on the time evolution of blend morphology during cooling, upon startup of shear flow, and upon cessation of shear flow (i.e., during stress relaxation). Among the important findings, we include the observation of an apparent flow-induced phase inversion from an isotropic matrix to a nematic matrix fluid, the existence of a lyotropic mesophase with a polymeric matrix, and evidence for a flow-induced isotropic-to-nematic phase transition in an isotropic/isotropic blend. In this study, we only have scratched the surface of the very complicated yet very important problem, scientifically and technologically, in the development of new polymeric materials by blending two TLCPs. A systematic investigation is worth pursuing in the future, to establish a firm scientific foundation, upon which new polymeric materials consisting of two TLCPs can be developed.

Acknowledgment. C.D.H. acknowledges that this study was supported in part by the National Science Foundation under Grant CTS-9614929. P.T.M. acknowledges partial support from the Air Force Office of Scientific Research under Grant F49620-00-1-0100.

References and Notes

(1) Watanabe, J.; Krigbaum, W. R. *Macromolecules* **1984**, *17*, 2288.
(2) Jin, J. H.; Choi, E. J.; Lee, K. Y. *Polym. J.* **1986**, *18*, 99.
(3) De Meuse, M., T.; Jaffe, M. *Mol. Cryst. Liq. Cryst.* **1988**, *157*, 535.
(4) Stachowski, M. J.; DiBenedetto, A. T. *Polym. Eng. Sci.* **1998**, *38*, 716.
(5) Chang, S.; Han, C. D. *Macromolecules* **1997**, *30*, 1670.
(6) Mather, P. T.; Stüber, H. R.; Chaffee, K. P.; Haddad, T. S.; Romo-Uribe, A.; Lichtenhan, J. D. *Mater. Res. Soc. Symp. Proc.* **1997**, *425*, 137.
(7) Mather, P. T.; Romo-Uribe, A.; Han, C. D.; Kim, S. S. *Macromolecules* **1997**, *30*, 7977.
(8) Hongladarom, K.; Burghardt, W. R.; Baek, S. G.; Cementwala, S.; Magda, J. J. *Macromolecules* **1993**, *26*, 772.
(9) Mather, P. T.; Jeon, H. G.; Han, C. D.; Chang, S. *Macromolecules* **2000**, *33*, 7595.
(10) Shiwaku, T.; Nakai, A.; Wang, W.; Hasegawa, H.; Hashimoto, T. *Liq. Cryst.* **1995**, *19*, 679.
(11) Chuang, I.; Turok, N.; Yurke, B. *Phys. Rev. Lett.* **1991**, *66*, 2472.
(12) Chuang, I.; Yurke, B.; Pargellis, A. N.; Turok, N. *Phys. Rev. E* **1993**, *47*, 3343.
(13) Chang, S.; Han, C. D. *Macromolecules* **1996**, *29*, 2103.
(14) Kim, S. S.; Han, C. D. *J. Rheol.* **1993**, *37*, 847.
(15) Kim, S. S.; Han, C. D. *Macromolecules* **1993**, *26*, 6633.
(16) Han, C. D.; Chang, S.; Kim, S. S. *Mol. Cryst. Liq. Cryst.* **1994**, *254*, 335.
(17) Han, C. D.; Kim, S. S. *J. Rheol.* **1994**, *38*, 13.
(18) Chang, S.; Han, C. D. *Macromolecule* **1997**, *30*, 2021.
(19) Kim, S. S.; Han, C. D. *J. Polym. Sci. Part B: Polym. Phys.* **1994**, *32*, 371.
(20) Kim, D. O.; Han, C. D.; Mather, P. T. *Macromolecules* **2000**, *33*, 7922.
(21) Minale, M.; Moldenaers, P.; Mewis, J. *J. Rheol.* **1999**, *43*, 815.
(22) Van Puyvelde, P.; Moldenaers, P.; Mewis, J.; Fuller, G. G. *Langmuir* **2000**, *16*, 3740.
(23) Gleeson, J. T.; Larson, R. G.; Mead, D. W.; Kiss, G.; Cladis, P. E. *Liq. Cryst.* **1992**, *11*, 341.
(24) Larson, R. G.; Mead, D. W. *Liq. Cryst.* **1992**, *12*, 751.
(25) Kricheldorf, H. R.; Wahlen, L. H.; Friedrich, C.; Menke, T. J. *Macromolecules* **1997**, *30*, 2642.

MA001964D